GENETICS

High-purity production and precise editing of DNA base editing ribonucleoproteins

Hyeon-Ki Jang[1†‡], Dong Hyun Jo[2†], Seu-Na Lee[3†], Chang Sik Cho[4], You Kyeong Jeong[1], Youngri Jung[1], Jihyeon Yu[1§], Jeong Hun Kim[4,5,6]*, Jae-Sung Woo[3]*, Sangsu Bae[1]*

Ribonucleoprotein (RNP) complex–mediated base editing is expected to be greatly beneficial because of its reduced off-target effects compared to plasmid- or viral vector–mediated gene editing, especially in therapeutic applications. However, production of recombinant cytosine base editors (CBEs) or adenine base editors (ABEs) with ample yield and high purity in bacterial systems is challenging. Here, we obtained highly purified CBE/ABE proteins from a human cell expression system and showed that CBE/ABE RNPs exhibited different editing patterns (i.e., less conversion ratio of multiple bases to single base) compared to plasmid-encoded CBE/ABE, mainly because of the limited life span of RNPs in cells. Furthermore, we found that off-target effects in both DNA and RNA were greatly reduced for ABE RNPs compared to plasmid-encoded ABE. We ultimately applied NG PAM–targetable ABE RNPs to in vivo gene correction in retinal degeneration 12 (*rd12*) model mice.

INTRODUCTION

DNA base editing tools, which include cytosine base editors (CBEs) and adenine base editors (ABEs), are capable of inducing precise base transitions with high efficacy. These tools, which are mainly composed of inactive Cas9 effectors fused with cytidine or adenosine deaminases, have key advantages: They rarely generate DNA double-strand breaks and do not require donor DNA templates (*1*, *2*). Thus, base editors have been widely used in a broad range of research areas including plant genome engineering (*3*–*6*), mouse zygote engineering (*7*, *8*), and biomedical applications (*9*–*13*). Recently, however, unexpected drawbacks have been reported. Similar to previously developed CRISPR nucleases, base editors also exhibit single-guide RNA (sgRNA)–dependent genome-wide off-target effects. ABEs have also been found to catalyze the conversion of cytosines, in addition to adenines, located in preferred sequence motifs (*14*). Furthermore, CBEs generate promiscuous, sgRNA-independent DNA deamination in the genome (*15*, *16*), and both CBEs and ABEs induce transcriptome-wide promiscuous RNA deamination in RNA transcripts (*17*–*19*). Attempts to minimize or mitigate those issues have included Cas9 effector engineering and the modification of cytidine and adenosine deaminases, but none of the issues have been completely resolved.

A complementary approach for reducing off-target effects is to modify another crucial variable: the means by which base editing tools are delivered. The intracellular delivery of bacterial plasmids or viral vectors that encode base editors and sgRNAs usually results in high off-target editing rates because the exogenous base editors are persistently produced and their intracellular concentrations are difficult to control; thus, off-target effects accumulate accordingly. In contrast, the delivery of base editor–sgRNA ribonucleoprotein (RNP) complexes can reduce off-target effects (*12*, *20*) because the RNPs are transiently active and rapidly degraded by endogenous cellular proteases (*21*). Furthermore, this method fundamentally avoids unexpected random integration of delivered DNAs and alleviates cellular immune responses mediated by excessive sgRNAs, increasing the safety of base editing. Previously, many advantages of RNP delivery were partly demonstrated for CBE in a sickle cell disease model (*13*) and for ABE in terms of reducing sgRNA-dependent or sgRNA-independent DNA off-target effects (*22*). Nonetheless, it has not been widely used for other biomedical applications, mainly because of the difficulty of producing high-quality base editor proteins. Previously, we used an *Escherichia coli* expression system to produce CBE and ABE but failed to obtain them at high purity and quantity (e.g., >99% purity and >1 mg per liter cell culture) due to the low level of expression of soluble full-length proteins, which consist of several different DNA/RNA binding proteins linked with long flexible linker peptides. In this study, we established a production system in human cells that yielded CBE/ABE proteins at high purity, investigated the on-target activities and off-target effects of RNPs for both DNA and RNA, and ultimately applied ABE RNPs to in vivo gene correction of the genetic defect in retinal degeneration 12 (*rd12*) model mice.

RESULTS

Base editor purification in a human cell expression system at high purity

To produce recombinant base editor proteins in a human cell system, we cloned the sequences encoding optimized versions of ABE and CBE, ABEmax and AncBE4max, respectively (*23*), into the mammalian expression vector pEX-FlagR. This vector is designed to fuse a red fluorescent protein (mCherry) and a double-affinity tag to the target protein to allow easy monitoring of protein expression and efficient protein purification, respectively (Fig. 1A and fig. S1). We transfected the resulting plasmids into human embryonic kidney

[1]Department of Chemistry and Research Institute for Convergence of Basic Sciences, Hanyang University, Seoul 04763, South Korea. [2]Department of Anatomy and Cell Biology, Seoul National University College of Medicine, Seoul 03080, South Korea. [3]Department of Life Sciences, Korea University, Seoul 02841, South Korea. [4]Fight against Angiogenesis-Related Blindness (FARB) Laboratory, Biomedical Research Institute, Seoul National University Hospital, Seoul 03080, South Korea. [5]Department of Ophthalmology, Seoul National University College of Medicine, Seoul 03080, South Korea. [6]Advanced Biomedical Research Center, Korea Research Institute of Bioscience & Biotechnology (KRIBB), Daejeon 34141, South Korea.
*Corresponding author. Email: steph25@snu.ac.kr (J.H.K.); jaesungwoo@korea.ac.kr (J.-S.W.); sangsubae@hanyang.ac.kr (S.B.)
†These authors contributed equally to this work.
‡Present address: Stem Cell Convergence Research Center, Korea Research Institute of Bioscience & Biotechnology (KRIBB), Daejeon 34141, South Korea.
§Present address: Division of Life Science, Korea Polar Research Institute, Incheon 21990, South Korea.

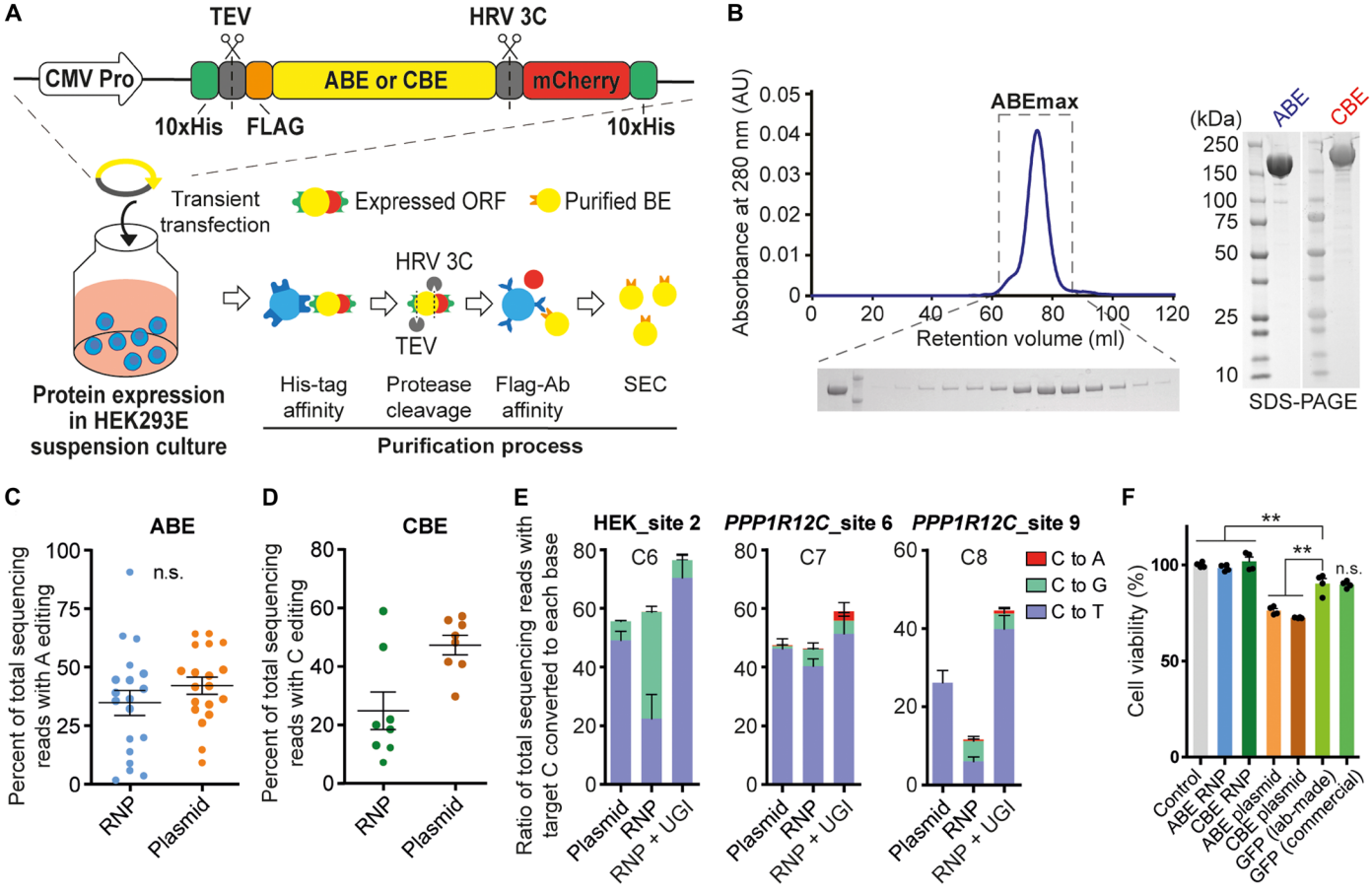

Fig. 1. Purification of ABE/CBE proteins in human cell expression system. (**A**) Schematic of base editor purification (see Materials and Methods). ORF, open reading frame. (**B**) Purified base editors. The peak fraction of ABEmax or AncBE4max from size exclusion chromatography (SEC) was collected, concentrated, and analyzed by SDS–polyacrylamide gel electrophoresis (PAGE). AU, absorbance unit. (**C** and **D**) Comparison of base editing frequencies after RNP- and plasmid-mediated ABE delivery (C) or CBE delivery (D). Dots represent the mean value of three independent biological replicates for each target. Error bars represent the SEM of the dots. (**E**) Percentage of sequencing reads with specific edited nucleotides that have been converted from target Cs in HEK293T cells after RNP- and plasmid-mediated CBE delivery with or without UGI overexpression. Cobalt, C to T; green, C to G; red, C to A. Error bars represent the SEM of three independent biological replicates. (**F**) Viability of HEK293T cells after RNP- and plasmid-mediated ABE/CBE delivery and GFP vectors. Viability was determined using a CCK-8 assay. Bars represent mean values, and error bars represent the SEM of three independent biological replicates. $^{**}P < 0.01$, comparing with the GFP (lab-made) by one-way analysis of variance (ANOVA) test with Dunnett's multiple comparison. n.s., not significant.

(HEK) 293E cells in a suspension culture and purified ABE/CBE proteins by sequentially using Ni affinity, anti–FLAG-M1 affinity, and size exclusion chromatography techniques. The polyhistidine and mCherry tags were removed by protease cleavage during purification; therefore, only the N-terminal FLAG tag remained on the purified ABE/CBE proteins. With this expression and purification method, we could reproducibly obtain 1 mg of highly purified CBE or ABE protein from a liter of cell culture (Fig. 1B).

We first sought to confirm the activities of the purified ABE/CBE proteins. To this end, we tested ABE RNPs targeting 19 different endogenous sites (*23*, *24*) and CBE RNPs targeting 8 different endogenous sites (*25*, *26*) in HEK293T cells. As a control, alternative delivery approach, we also transfected ABE/CBE-encoding plasmids. High-throughput sequencing data from bulk cell populations at 3 days after transfection indicated that ABE/CBE RNPs showed effective editing activities (Fig. 1, C and D, and fig. S2), indicating successful production of ABE/CBE proteins in our human cell system. It is notable that the overall ABE RNP activities were only slightly lower than those of plasmid-delivered ABEs (Fig. 1C), whereas CBE RNPs exhibited substantially lower activities than did plasmid-delivered CBEs (Fig. 1D and fig. S2E). CBEs include uracil DNA glycosylase inhibitor (UGI) to improve editing efficiency (*25*, *27*). Hence, we speculated that the concentration of UGI fused with CBE in RNPs was relatively lower than that in the plasmid-encoded version so that it was insufficient to inhibit uracil N-glycosylase activity in cells. When we additionally overexpressed UGI, the overall CBE RNP editing activity was enhanced and the ratio of products containing C-to-T edits to those containing any C edit was increased (Fig. 1E), confirming the speculation. We also found that both ABE and CBE RNPs were associated with better cell viability after transfection than were ABE- and CBE-encoding plasmids (Fig. 1F). When we transfected green fluorescent protein (GFP) vectors (~3.5 kb) as a control, mild decrease of cell viability was observed, indicating that the large size of ABE/CBE plasmids (~9 kb) might be the reason

of decreased cell viability, consistent with previous studies (*28*, *29*) reporting that large size of plasmids (6 to 16 kilo–base pairs) shows low viabilities and transfection efficiencies. These results also suggest that RNP systems would be suitable for further applications such as a medical treatment.

Editing activity windows and editing patterns of RNP- and plasmid-mediated ABE and CBE DNA editing

We next investigated whether we could discriminate the editing activity windows and editing patterns induced by ABE/CBE RNPs and by plasmid-encoded ABE/CBEs. An analysis of the editing outcomes in Fig. 1 (C and D) showed that the preferred editing activity windows of the RNPs and plasmid-encoded base editors were similar (fig. S2F), but the patterns of edits were different; RNPs generally converted fewer bases in an allele than did the plasmid-encoded editors. In the case of ABE_site 5, 47.8% of the products in ABE RNP–treated cells, but only 16.4% of the products in plasmid-treated cells, contained a single base conversion (Fig. 2A); multiple base conversions occurred more frequently via plasmid versus RNP delivery. This tendency was observed for most other targets (Fig. 2B) and also for CBEs (Fig. 2, C and D). To investigate the reason for the different editing outcomes, we measured the frequency of different editing patterns induced by plasmid-encoded ABEs at different time points (Fig. 2E). The ratio of multiple versus single base conversions gradually increased in a time-dependent manner (Fig. 2F), suggesting that prolonged expression of plasmid-encoded ABE is responsible for the conversion of multiple bases. In contrast, compared to plasmid-encoded ABE/CBEs, ABE/CBE RNPs generated fewer edits of bystander nucleotides, primarily because of their short life span in cells. For the remainder of our analysis, we mainly focused on ABEs rather than CBEs, because the characteristics of ABE proteins have not been thoroughly investigated to date.

To quantitate the amounts of ABE protein in cells resulting from the two different delivery methods, we transfected the ABE protein or ABE-encoding plasmid in the absence of sgRNAs and measured the ABE protein concentrations in cell lysates at different time points after transfection using Western blot assays. In the protein delivery experiment, the initial ABE protein concentration was maintained for 12 hours and was markedly decreased at 24 hours. However, in the case of plasmid delivery, the ABE concentration sharply increased until 6 hours, after which the maximum concentration was maintained until 24 hours. The concentration then slowly decreased for the next 6 days (Fig. 2G and fig. S3A). A comparison of the ABE protein abundance at each time point against the 6-hour time point in the plasmid-transfected cells showed that the protein delivery–induced ABE protein concentration was always less than the plasmid delivery–induced concentration except during the initial 3 hours under our experimental conditions (Fig. 2H). We further measured the ABE protein abundance in the presence of sgRNAs in cells after ABE RNP or ABE/sgRNA-encoding plasmid transfection (fig. S3, B and C). We found that overall tendency was similar to the above results without sgRNAs, but the ABE concentrations were more slowly decreased in both ABE RNP and plasmid delivery methods, probably because Cas9/sgRNA complexes are more stable than apo Cas9 proteins in cells (*30*).

RNP-, mRNA-, and plasmid-mediated DNA off-target effects of ABE at endogenous DNA sites

We next investigated DNA off-target effects following each delivery method. We first evaluated the sgRNA-dependent off-target DNA editing activity that is known to be caused by the Cas9 effector portion of ABE. In this experiment, we used mRNA delivery method (*31*) in addition to the RNP and plasmid delivery methods. mRNAs were in vitro transcribed, and sgRNAs were synthetized from Integrated DNA Technologies (IDT) Inc. To optimize the concentrations of ABE-encoding mRNA and sgRNA, we tested them with different doses for adenine base editing in HEK_site 2 and found the most efficient condition (i.e., 3.0 μg of each ABE-encoding mRNA and sgRNA) in HEK293T cells (fig. S4). For four defined targets (i.e., *HBG_site 3*, *HPRT_exon 8*, *VEGFA*, and HEK_site 4; table S2) (*24*, *32*, *33*), we assessed editing frequencies at both on-target and off-target sites after the transfection of ABE RNPs, ABE-encoding mRNAs, and ABE-encoding plasmids. High-throughput sequencing data showed that A-to-G conversion frequencies were markedly reduced at all off-target sites in RNP- and mRNA-transfected versus plasmid-transfected cells (Fig. 3A), even when RNP and mRNA delivery methods exhibited higher on-target DNA editing activities in *HPRT_exon 8* and *VEGFA* sites than the plasmid delivery method, similar to findings from previous studies (*12*, *22*).

Next, we examined the sgRNA-independent promiscuous DNA deamination activities for both ABEs or CBEs. To this end, we used an orthogonal R-loop assay by which single-stranded DNA regions could be formed with a catalytically inactive SaCas9 (dSaCas9) (Fig. 3B) (*22*, *34*). Results from the orthogonal R-loop assay showed that almost no A editing was detected at both R-loop site 5 and site 6 in ABE RNP–transfected cells, whereas a few rates of A editing were observed at the CA12G, CA9A, and AA10T motifs of both R-loop sites in ABE-encoding plasmid-transfected cells (Fig. 3C). Similar tendency but marked discrimination was observed in CBE RNP and CBE-encoding plasmid-transfected cells (Fig. 3D), consistent with previous findings (*34*). These results indicate that RNP delivery results in much more precise and specific base editing.

We further inspected the ABE-mediated cytosine deamination activity for ABE RNP and plasmid delivery methods. A previous study revealed that ABEs catalyze cytosine conversions in a narrow editing activity window (positions 5 to 7) and in a preferred TC*N sequence context (Fig. 3E). For a representative target site (*FANCF* target), we found that C conversions were commonly observed in both ABE RNP– and plasmid-transfected cells and that the ratio of C edit versus A edit was similar regardless of the delivery method (Fig. 3F). This result indicates that, to reduce the ABE-mediated C editing, further engineering of ABE would be necessary (*35*).

RNP-, mRNA-, and plasmid-mediated RNA off-target effects of ABE at RNA transcripts

We next investigated promiscuous ABE-mediated RNA deamination activities following each delivery method. To this end, we calculated adenine mutation frequencies in complementary DNAs (cDNAs) derived from well-defined RNA transcripts (*AARS1*, *RSL1D1*, and *TOPORS*; table S1) (*17*–*19*) at different time points after the transfection of ABE RNP, ABE-encoding mRNA, or ABE-encoding plasmids in the presence of sgRNAs targeting HEK_site 2. Notably, in RNP-transfected cells, ABE showed almost no RNA editing activities at the *AARS1* and *RSL1D1* sites at any time point and minor activity at the *TOPORS* site for the first 3 hours, whereas mRNA or plasmid-transfected cells showed the accumulation of promiscuous RNA deamination events at all three sites for more than 3 days (Fig. 4A). To examine that such RNA deamination activities are not related to the sgRNAs, we repeated the experiments in the absence

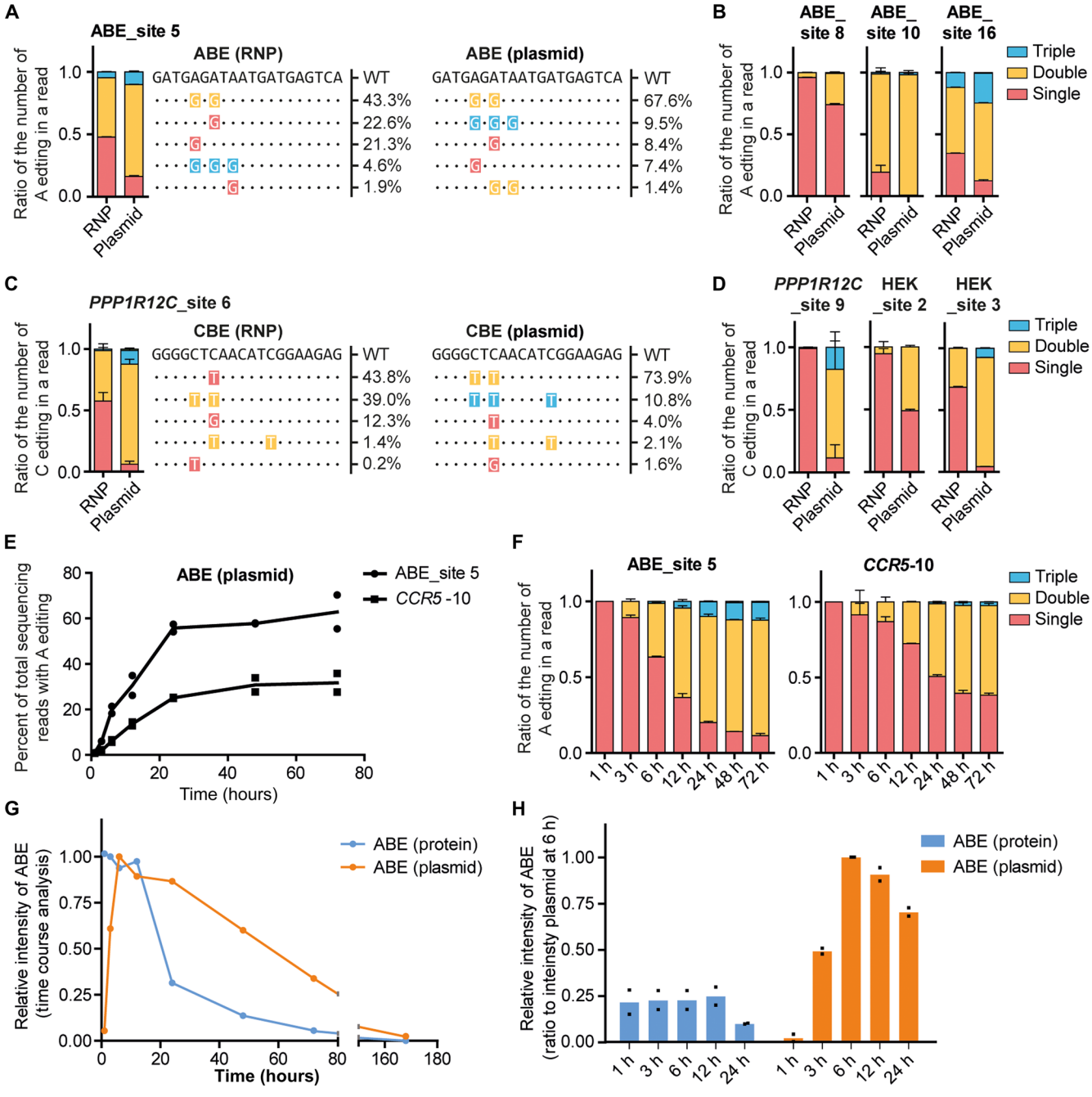

Fig. 2. RNP- and plasmid-mediated editing characteristics and at human endogenous DNA target sites. (**A** and **B**) Number of base conversions in ABE-edited alleles. Bars represent the ratio of the number of reads containing single (pink), double (yellow), or triple (blue) A conversions to the total number of reads containing A conversions. In (A), the five most common sequences (positions 1 to 20) at ABE_site 5 are visualized, with the frequency indicated to the right. Colored nucleotides represent edited sequences. (**C** and **D**) Number of base conversions in CBE-edited alleles at different target sites. Bars represent the ratio of the number of reads containing single (pink), double (yellow), or triple (blue) C conversions to the total number of reads containing C conversions. In (A) to (D), error bars represent the SEM of three independent biological replicates. (**E**) ABE editing efficiencies in HEK293T cells at different time points after transfection of the ABE-encoding plasmid. (**F**) Number of base conversions in ABE-edited alleles at different time points after transfection of the ABE-encoding plasmid. Error bars represent the SEM of two independent biological replicates. (**G** and **H**) Analysis of ABE abundance in HEK293T cells at different time points after transfection of the ABE protein (blue) or ABE-encoding plasmid (orange) in the absence of sgRNA. In (G), the points indicate the ABE abundance relative to the maximum abundance obtained for a given delivery method; in (H), the bars represent the ABE abundance relative to that obtained from plasmid-mediated expression at 6 hours after transfection. Dots (G) and bars (H) represent the mean value of two independent biological replicates.

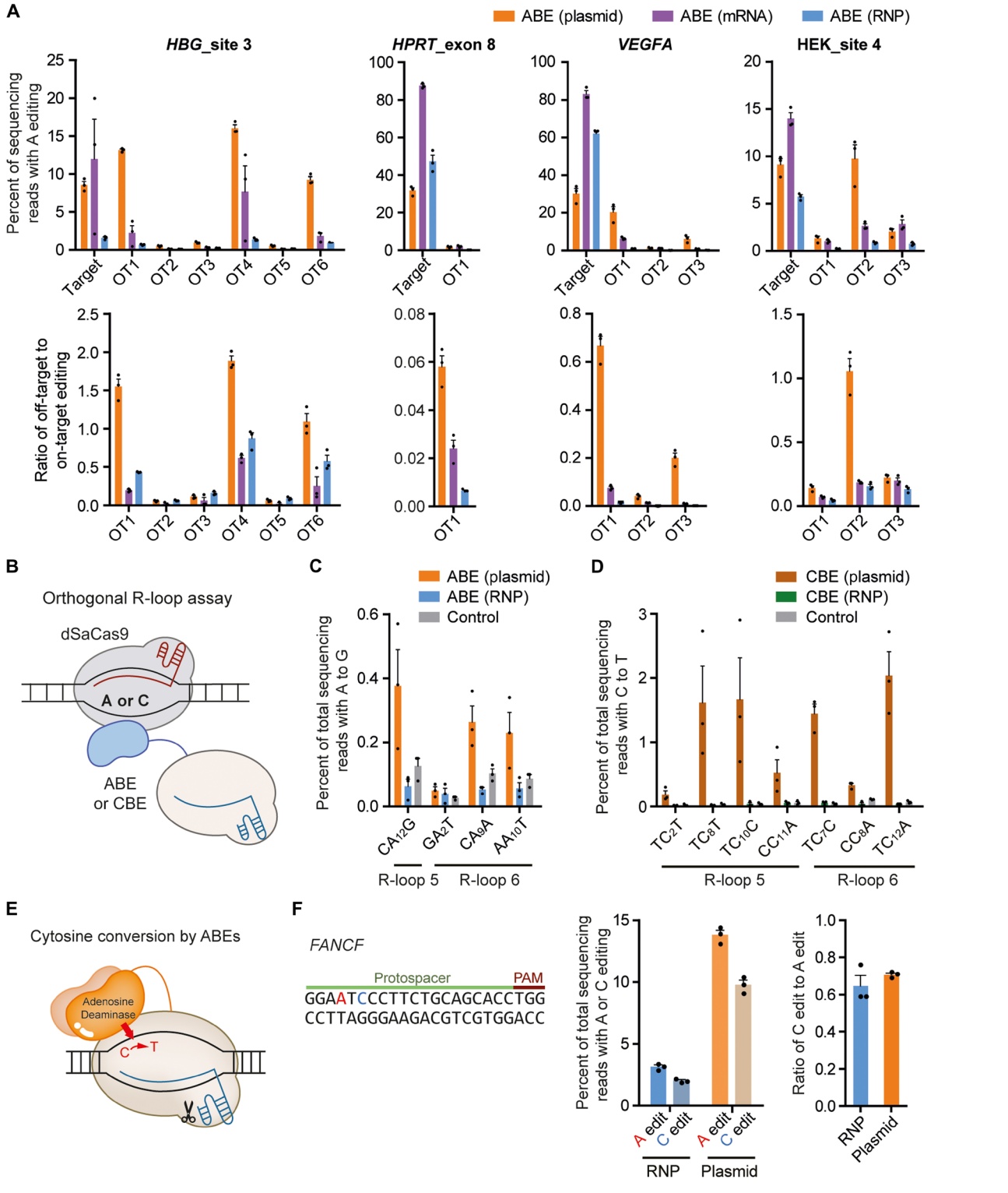

Fig. 3. Delivery-dependent variations in ABE-mediated DNA off-target effects. (**A**) Off-target DNA base editing in HEK293T cells after ABE RNP, ABE-encoding mRNA, and ABE-encoding plasmid delivery. A-to-G editing efficiencies (top) and the ratio of off-target over on-target A-to-G editing efficiencies (bottom) are shown. Bars represent mean values, and error bars represent the SEM of three independent biological replicates. (**B**) Overview of orthogonal R-loop assay. (**C** and **D**) sgRNA-independent off-target DNA editing frequencies detected by the orthogonal R-loop assay. Each R-loop was performed by cotransfection of ABE RNP or ABE-encoding plasmid in (C) and CBE RNP or CBE-encoding plasmid in (D) with HEK_site 2–targeting sgRNA and dSaCas9-encoding plasmid with SaCas9 sgRNA targeting R-loop 5 or 6. Bars represent mean values, and error bars represent the SEM of three independent biological replicates. (**E**) Overview of cytosine conversion by ABEs. (**F**) Editing efficiency of DNA C conversions in HEK293T cells after ABE RNP and ABE-encoding plasmid delivery was analyzed. Bars represent mean values, and error bars represent the SEM of three independent biological replicates.

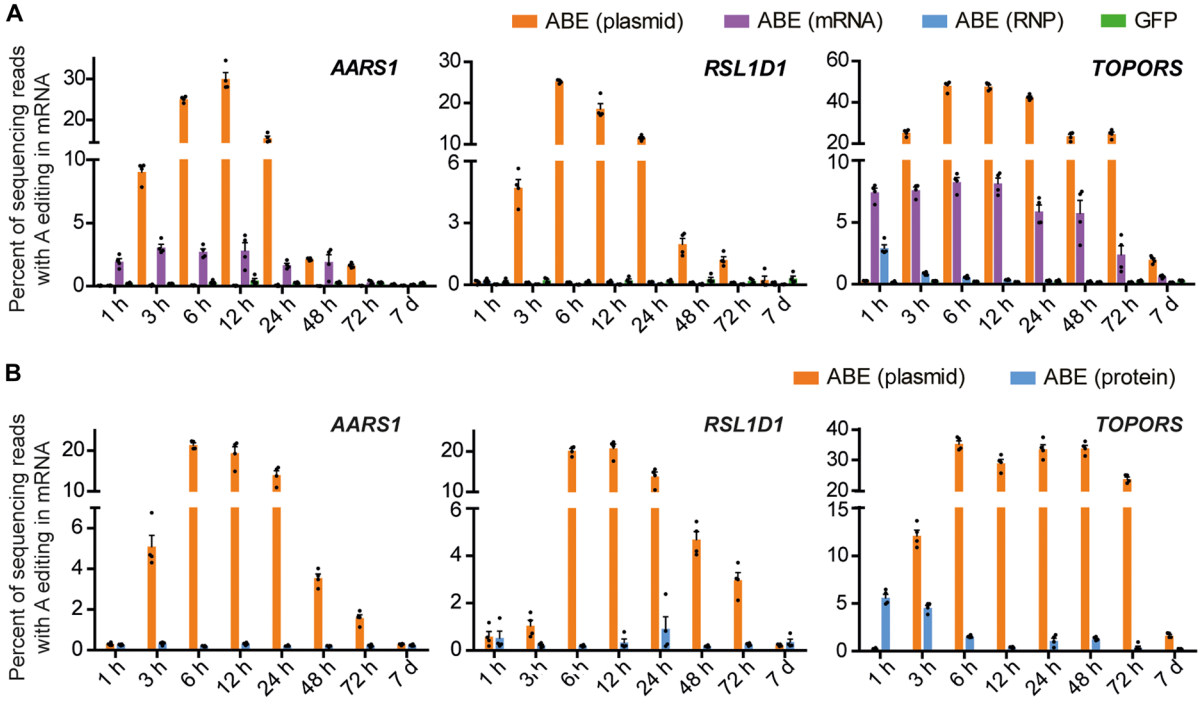

Fig. 4. Delivery-dependent variations in ABE-mediated RNA off-target effects. (**A**) Off-target RNA base editing in HEK293T cells after ABE RNP, ABE-encoding mRNA, and ABE-encoding plasmid delivery in the presence of sgRNA. Efficiencies of A-to-I mRNA editing are indicated. Delivery of a plasmid encoding GFP was used as a control. Bars represent mean values, and error bars represent the SEM of four independent biological replicates. (**B**) Off-target RNA base editing in HEK293T cells after ABE protein and ABE-encoding plasmid delivery in the absence of sgRNA. Efficiencies of A-to-I mRNA editing are indicated. Bars represent mean values, and error bars represent the SEM of four independent biological replicates.

of sgRNAs and found that the off-target RNA editing similarly occurred (Fig. 4B).

In vivo gene correction of the disease-associated mutation in *rd12* mice via NG-ABEmax RNP

To demonstrate biomedical application of ABE RNPs, we established in vivo DNA editing via ABE RNP delivery. As a proof of concept, we targeted *Fah* (*36*), *Vegfa* (*37*), and *Nr2e3* (*38*) genes in normal mice. The purified ABEmax and synthesized sgRNAs from IDT were injected together with Lipofectamine 2000 into one eye of adult mice via subretinal injection (fig. S5A). Genomic DNAs were isolated from retinal pigment epithelium (RPE) cells of RNP-injected mice at 1 week after injection and were subjected to the high-throughput sequencing data. The results showed clear base editing with average editing efficiencies of 1.7, 2.0, and 2.1% at *Fah*, *Vegfa*, and *Nr2e3*, respectively (fig. S5B).

Given the positive confidence, we tried to correct a nonsense mutation in the *Rpe65* gene that causes retinal degeneration in *rd12* mice. Because there was no relevant NGG (protospacer adjacent motif) PAM sequences near the mutation (Fig. 5A), we constructed a NG PAM–targetable ABEmax (hereafter NG-ABEmax) protein by incorporating seven additional mutations as previously done in SpCas9-NG (*39*). We then tested whether NG-ABEmax protein expressed in and purified from our human cell system would exhibit editing activity at six endogenous targets (*40*); high-throughput sequencing data showed editing at all six targets, proving the validity of our system for NG-ABEmax (fig. S5C). Then, we designed an sgRNA that included a TGA PAM and in which the disease-associated *Rpe65* point mutation (c.130C>T) matched an adenine at position 6 (A6) (Fig. 5A). We carefully tested the efficiency at which the mutation was corrected using NG-ABEmax RNPs with different forms of sgRNAs in embryonic fibroblasts from *rd12* mice (*rd12* mEFs) (Fig. 5B). We concluded that chemically synthesized sgRNA from IDT (X20_IDT) was associated with the most effective editing activity; hence, we also used it for in vivo delivery to mice.

We ultimately injected purified NG-ABEmax and synthesized X20_IDT sgRNA (hereafter target sgRNA) together with Lipofectamine 2000 into one eye of adult or juvenile *rd12* mice via subretinal injection (Fig. 5C). We found that injected NG-ABEmax RNPs had successfully localized in the cytosol and nucleus in cells in the RPE at 6 hours after the injection (Fig. 5D), whereas NG-ABEmax RNPs were not detectable in the RPE at 72 hours after the injection (fig. S6A), indicating that RNPs were rapidly degraded in cells in vivo as they were in cultured cells (Fig. 2G). Notably, high-throughput sequencing data from genomic DNA isolated from the RPE of NG-ABEmax RNP–injected mice showed precise correction of the *rd12* mutation without detectable bystander editing (fig. S6B). The average correction efficiencies were 1.8% in juvenile (Fig. 5E) and 1.2% in adult mice (fig. S6C), which is comparable to the level of homology-directed repair-mediated correction induced by Cas9 delivered by an adeno-associated viral vector in our previous study (*41*). The maximum correction efficiency that we observed in this study was 5.7% in a juvenile mouse. The recovery of a functional *Rpe65* gene was validated at both the mRNA and protein levels. We observed a significant increase in *Rpe65* mRNA expression in the RPE of *rd12* mice treated with ABE RNPs that included the target sgRNA; in

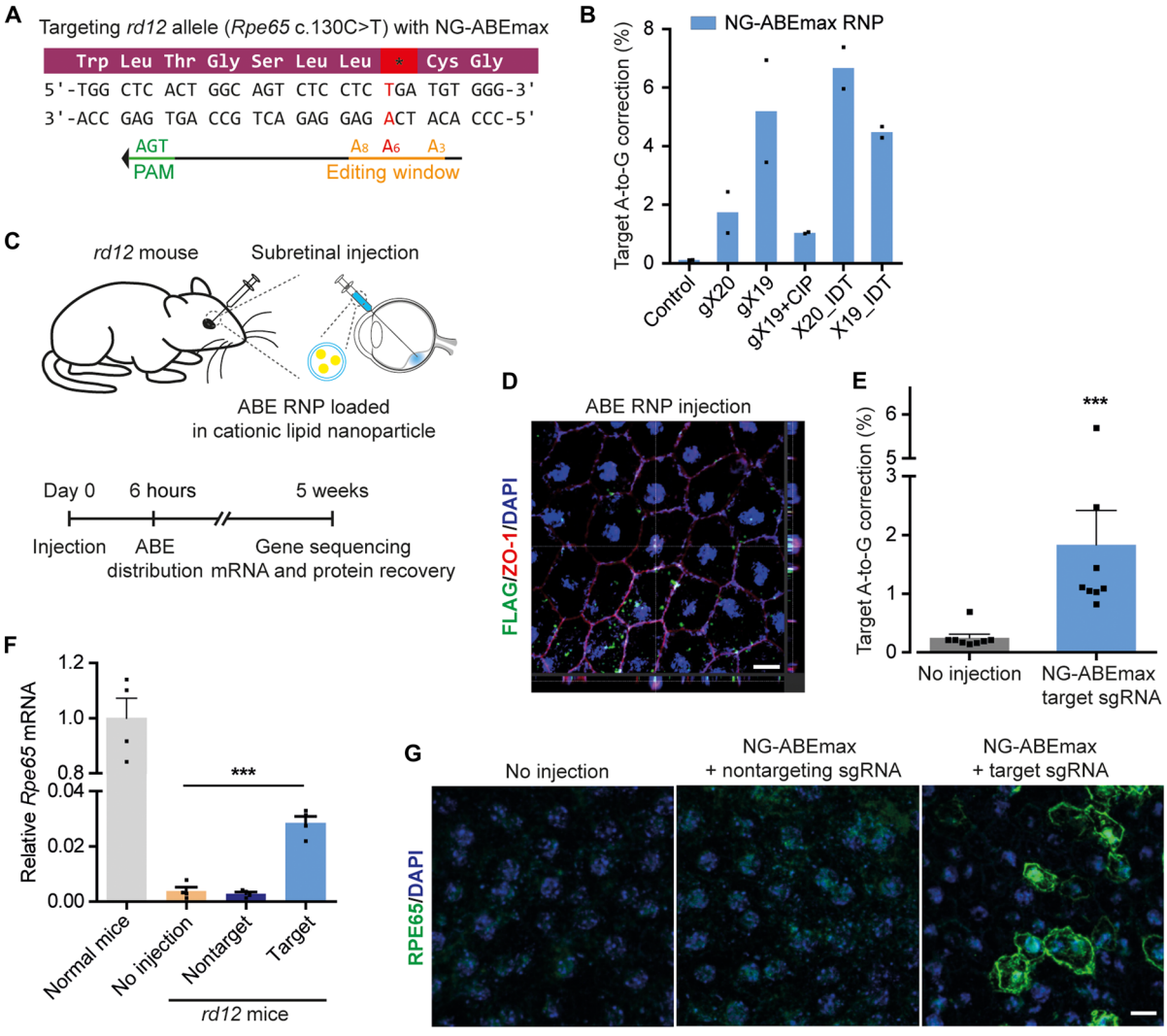

Fig. 5. NG-ABEmax RNP–mediated correction of the disease-associated mutation in *rd12* mice. (**A**) Strategy for NG-ABEmax RNP–mediated correction of the nonsense mutation in *Rpe65* in *rd12* mice. (**B**) Efficiencies of NG-ABEmax RNP–mediated mutation corrections in *rd12* mEFs using different sgRNAs. Control, NG-ABEmax without sgRNA. Bars represent the mean values of two independent replicates. gX19 and gX20, in vitro transcribed sgRNAs, with mismatched 5′ Gs, containing 19- and 20-nucleotide (nt) spacers, respectively; X19 and X20, chemically synthesized sgRNAs containing 19 and 20 nt spacers, respectively. (**C**) Schematic of NG-ABEmax RNP–mediated treatment of *rd12* mice via subretinal injections. RNPs (yellow circles) were encapsulated into cationic lipid nanoparticles. (**D**) Representative confocal micrograph of RPE from *rd12* mice at 6 hours after injection. Scale bar, 10 μm. DAPI, 4′,6-diamidino-2-phenylindole. (**E**) Efficiencies of NG-ABEmax RNP–mediated mutation corrections in *rd12* mice ($n = 8$). Genomic DNAs from RPE from eyes injected or not with NG-ABEmax RNPs were analyzed to determine target A-to-G editing efficiencies. Bars represent mean values, and error bars represent the SEM of the eight independent replicates. ***$P < 0.001$ by Mann-Whitney test. (**F**) Relative expression of *Rpe65* mRNA in RPE from *rd12* mice injected with NG-ABEmax RNPs ($n = 4$). (**G**) Representative confocal micrographs of the RPE from *rd12* mice at 5 weeks after injection. Scale bars, 10 μm. ***$P < 0.001$ by Kruskal-Wallis test with Dunn's multiple comparison tests. Nontarget, *rd12* mice injected with NG-ABEmax RNPs including nontargeting sgRNA; Target, *rd12* mice injected with NG-ABEmax RNPs including target sgRNA.

these mice, the expression level was 2.8% of that in normal mice, which was significantly higher than the level in untreated *rd12* mice or in *rd12* mice treated with ABE RNPs that included a nontargeting sgRNA (Fig. 5F). In addition, we found that RPE65 was expressed in the RPE of NG-ABEmax RNP–treated *rd12* mice (Fig. 5G), showing the successful rescue of mutant *Rpe65* via gene correction.

DISCUSSION

In this study, we produced CBE/ABE proteins in human cells; our method resulted in ample yields of purified proteins. We showed that CBE/ABE RNPs were associated with different editing patterns (i.e., fewer base conversions in each allele) than were plasmid-encoded CBE/ABEs, mainly because of their short life span in cells. Furthermore, we found that delivery of ABE RNPs strongly reduced off-target DNA and RNA effects compared to delivery of plasmid-encoded ABEs. We used NG-ABEmax RNPs to induce in vivo gene correction in *rd12* model mice.

Our optimized protocol for ABE purification from human cells yields 1 to 2 mg of highly purified protein per liter of suspension cell culture. This good yield enabled multiple tests using ABE RNPs, including analyses of on-target editing at 19 genomic sites in cells

and in vivo editing of the disease-causing mutation in *rd12* mice. Previous studies have limited tests using ABE RNPs to in vitro studies or to a few genomic sites in cells, mainly for the analysis of DNA off-target editing (*22*, *32*, *33*). Our results should broaden understanding of the characteristics of RNP-mediated ABE editing, including bystander editing patterns and off-target editing, and provide insight into how these features differ from those of plasmid-encoded ABE. We further showed that ABE RNP–mediated editing is more specific than mRNA-mediated editing in terms of RNA off-target editing, although both RNP- and mRNA-mediated editing showed reduced DNA off-target editing compared to plasmid-mediated editing. Unlike the situation with ABE, the therapeutic potential of CBE RNP delivery has been demonstrated in vivo (*12*, *42*) and ex vivo (*13*). A recent study showed efficient ex vivo editing with high-dose (40 μM) treatment with CBE (*13*); in this approach, it was estimated that about 160 μg of CBE protein was used to treat 50,000 hematopoietic stem and progenitor cells. To date, however, the use of RNPs for ABE delivery for biomedical applications has been limited, although delivery via mRNA (*31*), plasmid (*43*), and viral vector (*9*, *10*, *44*) has demonstrated the therapeutic potential of ABE, including a recent study showing successful gene correction of the rd12 mutation and restoration of retinal function in *rd12* mice using ABE-encoding lentiviral vector (*45*). To the best of our knowledge, our use of RNP-mediated ABE delivery for in vivo gene correction in mice is the first biomedical application of ABE RNPs.

To improve the therapeutic efficacy of ABE RNPs, the latest versions of ABE, ABE8s (*46*) or ABE8e (*22*), should be used in further studies. The relatively weak binding affinity of SpCas9-NG for target DNA and the short life span of RNPs in cells might explain the lower activity of NG-ABE delivered via RNPs versus plasmids, which could be improved by using the newly evolved ABEs. We found that NGG-ABE RNP showed apparently better in vivo editing activity compared to NG-ABE RNP (fig. S6D), but more marked improvement would be necessary for therapeutic use. This issue could be addressed in the future by adopting ABE8e showing faster reaction kinetics. We envision that RNP delivery of ABE8s or ABE8e, together with appropriate modifications to reduce off-target editing, will be a promising method for improved on-target editing with negligible off-target DNA and RNA editing.

MATERIALS AND METHODS

Plasmid construction

To construct pEX-FlagR-ABEmax and pEX-FlagR-BE4max, the ABEmax and BE4max coding sequences (CDSs) were amplified from pCMV_ABEmax (Addgene no.112095) and pCMV_AncBE4max (Addgene no. 112094), respectively, and cloned into the mammalian expression pEX-FlagR vector using the Xho I and Xba I restriction sites. To construct pCMV-NGABEmax, we replaced the Cas9 sequence in pCMV_ABEmax with the SpCas9-NG sequence from pX330-SpCas9-NG (Addgene no. 117919) using the Pml I and Eco RI restriction sites. To construct pEX-FlagR-NGABEmax, the NGABEmax sequence from pCMV-NGABEmax was cloned into pEX-FlagR. Gibson fragments containing the ABEmax or BE4max CDS with matching overlaps were polymerase chain reaction (PCR)–amplified using Phusion High-Fidelity DNA Polymerase [New England Biolabs (NEB)]. Fragments were gel-purified and assembled using NEBuilder HiFi DNA Assembly master mix (NEB) for 1 hour at 50°C and transformed into chemically competent *E. coli* (DH5α; Enzynomics). Sequences corresponding to sgRNAs were cloned into Bsa I–digested pRG2 vector (Addgene no. 104174). For this step, oligos containing the spacer sequence (table S3) were annealed to form double-stranded DNA fragments with compatible overhangs and ligated using T4 ligase (Enzynomics). All plasmids used for transfection experiments were prepared using a NucleoBond Xtra Midi Plus EF kit [Macherey-Nagel (MN)].

Protein expression and purification

HEK293E cells were grown at 37°C in suspension in Dulbecco's modified Eagle's medium (DMEM) with glucose (4500 mg/liter) without calcium (WELGENE) supplemented with 5% fetal bovine serum (FBS). For overexpression of the base editors (ABEmax or BE4max), HEK293E cells were transiently transfected with pEX-FlagR-ABEmax (NG PAM or NGG PAM) or pEX-FlagR-AncBE4max (NGG PAM) plasmids, which were designed to express each base editor as a fusion protein with a 10xHis-Flag tag at the N terminus and an mCherry-10xHis tag at the C terminus. Cells were transfected at a density of 7×10^5 cells/ml with 25-kDa linear polyethylenimine (Polysciences). Dimethyl sulfoxide (Amresco) was added immediately after the transfection to a final concentration of 1%, and the temperature was lowered to 33°C. Two days after transfection, tryptone (Amresco) was added to a final concentration of 0.5%. Four days after transfection, the cells were harvested at 500*g* for 20 min and resuspended in lysis buffer [20 mM tris-HCl (pH 7.5), 1 M NaCl, and 2 mM β-mercaptoethanol] supplemented with 20% glycerol. The resuspended cells were lysed by sonication. The resulting solution was centrifuged, and the supernatant was loaded on a Ni-NTA column (Qiagen). After the column was washed with buffer A [20 mM tris-HCl (pH 7.5), 500 mM NaCl, 2 mM β-mercaptoethanol, and 20% glycerol] supplemented with 40 mM imidazole (MilliporeSigma), the bound proteins were eluted with buffer A supplemented with 200 mM imidazole. The eluted proteins were treated with tobacco etch virus (TEV) protease and human rhinovirus (HRV) 3C protease overnight to expose the FLAG tag at the N terminus and to remove the C-terminal mCherry-10xHis tag, respectively. The sample was mixed with α-FLAG M1 agarose resin (MilliporeSigma) in the presence of 5 mM $CaCl_2$ with slow rotation at 4°C for 1 hour. After a wash with buffer A supplemented with 1 mM $CaCl_2$, the bound proteins were eluted with buffer A supplemented with 5 mM EGTA. The eluted FLAG-ABEmax (or FLAG-CBEmax) was concentrated and further purified using a HiLoad 16/600 Superdex 200-pg column equilibrated with a buffer containing 20 mM tris-HCl (pH 7.5), 500 mM NaCl, 1 mM β-mercaptoethanol, and 20% glycerol (storage buffer). The peak fraction was concentrated to ~10 mg/ml, flash-frozen in liquid nitrogen, and stored at −80°C.

Guide RNA preparation

For RNP delivery of base editors, sgRNAs were synthesized by in vitro transcription using T7 RNA polymerase and a template oligonucleotide (table S4). In vitro transcribed sgRNA targeting the *rd12* allele was additionally treated with calf intestinal alkaline phosphatase (CIP; NEB) to remove the 5′-triphosphate (gX19 + CIP), as described previously (*47*). Chemically synthesized sgRNAs targeting the *rd12* allele (X19_IDT and X20_IDT), which contain chemical modifications (Alt-R sgRNA), were purchased from IDT Inc.

ABE-encoding mRNA preparation

pCMV_ABEmax was linearized by digestion with Pme I and used as a template for in vitro synthesis of ABE-encoding mRNA.

ABE-encoding mRNA was transcribed by using the mMESSAGE mMACHINE T7 Transcription Kit (Invitrogen) and cotranscriptionally capped at the 5′ end to produce 7-methylguanosine–capped mRNA. Then, the 3′ termini of the mRNA were polyadenylated by the Poly(A) Tailing Kit (Invitrogen) according to the manufacturer's instructions.

Cell culture and transfection for base editing experiments

HEK293T cells (American Type Culture Collection CRL-11268) were cultured in DMEM supplemented with 10% FBS and 1% penicillin-streptomycin (WELGENE). For ABE or CBE RNP–mediated genome editing, 15 μg of base editor protein [ABE (10 mg/ml) or CBE (8 mg/ml) dissolved in storage buffer] and 8 μg of in vitro transcribed or chemically synthesized sgRNA were mixed and incubated for 10 min at room temperature for the RNP complex formation. Then, the RNP complex was mixed with HEK293T cells (1.5×10^5) and electroporated via the Neon Transfection System. For ABE RNP–mediated RNA off-target editing and time course analysis, HEK293T cells (1.5×10^5) were electroporated as above without sgRNA. For ABE- or CBE-encoding plasmid-mediated genome editing, ABE- or CBE-encoding plasmids (0.5 μg) and sgRNA-encoding plasmids (0.17 μg) were mixed with HEK293T cells (1.5×10^5) and electroporated using the Neon Transfection System. For optimization of ABE-encoding mRNA–meditated genome editing, ABE-encoding mRNA (3.0 μg) and different doses of sgRNAs (0.6, 1.5, 3.0, 8.0, or 16.0 μg) were mixed with HEK293T cells (1.5×10^5) and electroporated using the Neon Transfection System.

For orthogonal R-loop assay with base editor plasmid, 500 ng of dead SaCas9 plasmid (Addgene no. 138162), 170 ng of SaCas9 sgRNA plasmid, 500 ng of base editor plasmid, and 170 ng of base editor sgRNA plasmid were cotransfected into HEK293T cells (1.0×10^5) using 2 μl of Lipofectamine 2000 (catalog no. 11668019; Thermo Fisher Scientific). For orthogonal R-loop assay with base editor RNP, 500 ng of dead SaCas9 plasmid, 170 ng of SaCas9 sgRNA plasmid, and 670 ng of pUC19 plasmid (negative control plasmid) were cotransfected into HEK293T cells (1.0×10^5) using 2 μl of Lipofectamine 2000. One day after transfection, cells treated without base editor plasmid were trypsinized and centrifuged for 8 min at 100*g*. After resuspending the cells, the cells were electroporated with base editor protein (15 μg) and in vitro transcribed sgRNA (8 μg) using the Neon Transfection System.

For the correction of rd12 mutation in vitro, mEFs from *rd12* mice were maintained in DMEM supplemented with 10% FBS, 1% penicillin-streptomycin (WELGENE), and 4 mM glutamine (GlutaMAX I, Gibco). For ABE RNP–mediated gene correction, mEFs (1.5×10^5) were electroporated with NGABEmax protein (15 μg) and in vitro transcribed sgRNA (8 μg), CIP-treated in vitro transcribed sgRNA (8 μg), or chemically synthesized sgRNA (8 μg; IDT) using the Neon Transfection System.

Western blots

Cell lysates were prepared from ABE-transfected HEK293T cells at the indicated time points using radioimmunoprecipitation assay buffer (Sigma-Aldrich) supplemented with Protease inhibitor cocktails (Sigma-Aldrich). Protein concentrations were measured using a bicinchoninic acid assay kit (Thermo Fisher Scientific). Equal amounts of proteins were loaded onto Mini-PROTEAN TGX Protein Gels (Bio-Rad) and run at 80 V for 20 min and 120 V for 40 min. After the proteins were transferred to a nitrocellulose membrane, the blots were incubated with anti-Cas9 (#844301, BioLegend) and anti-tubulin (#3873, Cell Signaling Technology) antibodies, followed by incubation with appropriate horseradish peroxidase (HRP)–conjugated secondary antibodies (#7076, Cell Signaling Technology). The chemiluminescence from HRP reaction was detected using a Fusion SL gel chemiluminescence documentation system (Vilber Lourmat).

Animals

Eight-week-old male C57BL/6 mice and mating pairs of *rd12* mice (stock no. 005379, The Jackson Laboratory) were purchased through Central Laboratory Animal and maintained under a 12-hour dark-light cycle. All animal experiments were performed in accordance with guidelines from the Association for Research in Vision and Ophthalmology statement for the use of animals in ophthalmic and vision research. The Institutional Animal Care and Use Committees of both Seoul National University and Seoul National University Hospital approved the protocols.

Subretinal injections

Three-week-old mice (juvenile mice) or 6-month-old mice (adult mice) were anesthetized. The mice then received a subretinal injection of a 1:1 (v/v) mixture of RNP and Lipofectamine 2000 (catalog no. 11668019, Thermo Fisher Scientific) in one eye using a customized NanoFil syringe with a 33-gauge blunt needle (World Precision Instruments), as previously described (*48*). Each dose included 12.54 μg of NG-ABEmax and 5.76 μg of the appropriate sgRNA. The total volume was 3 μl per eye.

Targeted deep sequencing

For analysis of DNA or RNA on-target and off-target sites, genomic DNA or total RNAs were extracted from ABE-transfected cells using a NucleoSpin Tissue kit (MN) or NucleoSpin RNA Plus kit (MN) at the indicated time points or at 3 days after transfection. cDNAs were synthesized from the RNAs using PrimeScript RT Master Mix (Takara). In preparation for sequencing of ABE-targeted sites in normal or *rd12* mice, genomic DNA was extracted from RPE cells using a NucleoSpin Tissue kit (MN) at 1 or 5 weeks after subretinal injection of the ABE RNP/Lipofectamine 2000 mixture. On-target and off-target sites were amplified using a KOD Multi & Epi PCR kit (TOYOBO) for sequencing library generation (tables S5 and S6 for the primer sequences). These libraries were sequenced using MiniSeq with a TruSeq HT Dual Index system (Illumina) as previously described (*49*). Briefly, equal amounts of the PCR amplicons were subjected to paired-end read sequencing using an Illumina MiniSeq platform. After MiniSeq, paired-end reads were analyzed by comparing wild-type and mutant sequences using BE-Analyzer (*50*).

Immunofluorescence

At the indicated time points after the subretinal injection, mice were sacrificed and RPE-choroid-scleral complexes were prepared. The complexes were then treated with anti-FLAG (catalog no. MA1-142-A488, Thermo Fisher Scientific), anti–ZO-1 (catalog no. 339194, Thermo Fisher Scientific), or anti-RPE65 (catalog no. NB100-355AF488, Novus Biologicals) antibodies and observed under a confocal microscope. The nuclei were identified using 4′,6-diamidino-2-phenylindole (catalog no. D9542, Sigma-Aldrich).

Quantitative RT-PCR

Total RNAs were prepared from RPE cells with TRIzol reagent (catalog no. 15596018, Thermo Fisher Scientific) at 5 weeks after subretinal

injection of the ABE RNP/Lipofectamine 2000 mixture. The qualities and quantities of the extracted RNAs were evaluated with the NanoDrop 2000 Spectrophotometer (Thermo Fisher Scientific). cDNAs were prepared with a High-Capacity RNA-to-cDNA kit (catalog no. 4387406, Thermo Fisher Scientific). Quantitative RT-PCR was performed with the StepOnePlus Real-Time PCR System (Thermo Fisher Scientific) using TaqMan Fast Advanced Master Mix (catalog no. 4444556, Thermo Fisher Scientific) and Gene Expression Assays (Thermo Fisher Scientific). Product IDs of the gene expression assays are as follows: for *Rpe65*, Mm00504133_m1; for *Gapdh*, Mm99999915_g1; and for *Rn18s*, Mm03928990_g1. The relative *Rpe65* gene expression levels were normalized to those of *Gapdh* and *Rn18s*. All procedures were performed in accordance with the Minimum Information for Publication of Quantitative Real-Time PCR Experiments guidelines.

SUPPLEMENTARY MATERIALS

Supplementary material for this article is available at http://advances.sciencemag.org/cgi/content/full/7/35/eabg2661/DC1

View/request a protocol for this paper from *Bio-protocol*.

REFERENCES AND NOTES

1. H.-K. Jang, B. Song, G.-H. Hwang, S. Bae, Current trends in gene recovery mediated by the CRISPR-Cas system. *Exp. Mol. Med.* **52**, 1016–1027 (2020).
2. Y. K. Jeong, B. Song, S. Bae, Current status and challenges of DNA base editing tools. *Mol. Ther.* **28**, 1938–1952 (2020).
3. B.-C. Kang, J.-Y. Yun, S.-T. Kim, Y. Shin, J. Ryu, M. Choi, J. W. Woo, J.-S. Kim, Precision genome engineering through adenine base editing in plants. *Nat. Plants* **4**, 427–431 (2018).
4. Y. Zong, Y. Wang, C. Li, R. Zhang, K. Chen, Y. Ran, J.-L. Qiu, D. Wang, C. Gao, Precise base editing in rice, wheat and maize with a Cas9-cytidine deaminase fusion. *Nat. Biotechnol.* **35**, 438–440 (2017).
5. Z. Shimatani, S. Kashojiya, M. Takayama, R. Terada, T. Arazoe, H. Ishii, H. Teramura, T. Yamamoto, H. Komatsu, K. Miura, H. Ezura, K. Nishida, T. Ariizumi, A. Kondo, Targeted base editing in rice and tomato using a CRISPR-Cas9 cytidine deaminase fusion. *Nat. Biotechnol.* **35**, 441–443 (2017).
6. C. Li, Y. Zong, Y. Wang, S. Jin, D. Zhang, Q. Song, R. Zhang, C. Gao, Expanded base editing in rice and wheat using a Cas9-adenosine deaminase fusion. *Genome Biol.* **19**, 59 (2018).
7. K. Kim, S.-M. Ryu, S.-T. Kim, G. Baek, D. Kim, K. Lim, E. Chung, S. Kim, J.-S. Kim, Highly efficient RNA-guided base editing in mouse embryos. *Nat. Biotechnol.* **35**, 435–437 (2017).
8. P. Liang, H. Sun, Y. Sun, X. Zhang, X. Xie, J. Zhang, Z. Zhang, Y. Chen, C. Ding, Y. Xiong, W. Ma, D. Liu, J. Huang, Z. Songyang, Effective gene editing by high-fidelity base editor 2 in mouse zygotes. *Protein Cell* **8**, 601–611 (2017).
9. L. Villiger, H. M. Grisch-Chan, H. Lindsay, F. Ringnalda, C. B. Pogliano, G. Allegri, R. Fingerhut, J. Häberle, J. Matos, M. D. Robinson, B. Thöny, G. Schwank, Treatment of a metabolic liver disease by in vivo genome base editing in adult mice. *Nat. Med.* **24**, 1519–1525 (2018).
10. S.-M. Ryu, T. Koo, K. Kim, K. Lim, G. Baek, S.-T. Kim, H. S. Kim, D.-e. Kim, H. Lee, E. Chung, J.-S. Kim, Adenine base editing in mouse embryos and an adult mouse model of Duchenne muscular dystrophy. *Nat. Biotechnol.* **36**, 536–539 (2018).
11. W.-H. Yeh, O. Shubina-Oleinik, J. M. Levy, B. Pan, G. A. Newby, M. Wornow, R. Burt, J. C. Chen, J. R. Holt, D. R. Liu, In vivo base editing restores sensory transduction and transiently improves auditory function in a mouse model of recessive deafness. *Sci. Transl. Med.* **12**, eaay9101 (2020).
12. H. A. Rees, A. C. Komor, W.-H. Yeh, J. Caetano-Lopes, M. Warman, A. S. B. Edge, D. R. Liu, Improving the DNA specificity and applicability of base editing through protein engineering and protein delivery. *Nat. Commun.* **8**, 15790 (2017).
13. J. Zeng, Y. Wu, C. Ren, J. Bonanno, A. H. Shen, D. Shea, J. M. Gehrke, K. Clement, K. Luk, Q. Yao, R. Kim, S. A. Wolfe, J. P. Manis, L. Pinello, J. K. Joung, D. E. Bauer, Therapeutic base editing of human hematopoietic stem cells. *Nat. Med.* **26**, 535–541 (2020).
14. H. S. Kim, Y. K. Jeong, J. K. Hur, J.-S. Kim, S. Bae, Adenine base editors catalyze cytosine conversions in human cells. *Nat. Biotechnol.* **37**, 1145–1148 (2019).
15. E. Zuo, Y. Sun, W. Wei, T. Yuan, W. Ying, H. Sun, L. Yuan, L. M. Steinmetz, Y. Li, H. Yang, Cytosine base editor generates substantial off-target single-nucleotide variants in mouse embryos. *Science* **364**, 289–292 (2019).
16. S. Jin, Y. Zong, Q. Gao, Z. Zhu, Y. Wang, P. Qin, C. Liang, D. Wang, J.-L. Qiu, F. Zhang, C. Gao, Cytosine, but not adenine, base editors induce genome-wide off-target mutations in rice. *Science* **364**, 292–295 (2019).
17. J. Grünewald, R. Zhou, S. P. Garcia, S. Iyer, C. A. Lareau, M. J. Aryee, J. K. Joung, Transcriptome-wide off-target RNA editing induced by CRISPR-guided DNA base editors. *Nature* **569**, 433–437 (2019).
18. C. Zhou, Y. Sun, R. Yan, Y. Liu, E. Zuo, C. Gu, L. Han, Y. Wei, X. Hu, R. Zeng, Y. Li, H. Zhou, F. Guo, H. Yang, Off-target RNA mutation induced by DNA base editing and its elimination by mutagenesis. *Nature* **571**, 275–278 (2019).
19. H. A. Rees, C. Wilson, J. L. Doman, D. R. Liu, Analysis and minimization of cellular RNA editing by DNA adenine base editors. *Sci. Adv.* **5**, eaax5717 (2019).
20. J. A. Zuris, D. B. Thompson, Y. Shu, J. P. Guilinger, J. L. Bessen, J. H. Hu, M. L. Maeder, J. K. Joung, Z. Y. Chen, D. R. Liu, Cationic lipid-mediated delivery of proteins enables efficient protein-based genome editing in vitro and in vivo. *Nat. Biotechnol.* **33**, 73–80 (2015).
21. S. Kim, D. Kim, S. W. Cho, J. Kim, J.-S. Kim, Highly efficient RNA-guided genome editing in human cells via delivery of purified Cas9 ribonucleoproteins. *Genome Res.* **24**, 1012–1019 (2014).
22. M. F. Richter, K. T. Zhao, E. Eton, A. Lapinaite, G. A. Newby, B. W. Thuronyi, C. Wilson, L. W. Koblan, J. Zeng, D. E. Bauer, J. A. Doudna, D. R. Liu, Phage-assisted evolution of an adenine base editor with improved Cas domain compatibility and activity. *Nat. Biotechnol.* **38**, 883–891 (2020).
23. L. W. Koblan, J. L. Doman, C. Wilson, J. M. Levy, T. Tay, G. A. Newby, J. P. Maianti, A. Raguram, D. R. Liu, Improving cytidine and adenine base editors by expression optimization and ancestral reconstruction. *Nat. Biotechnol.* **36**, 843–846 (2018).
24. N. M. Gaudelli, A. C. Komor, H. A. Rees, M. S. Packer, A. H. Badran, D. I. Bryson, D. R. Liu, Programmable base editing of A•T to G•C in genomic DNA without DNA cleavage. *Nature* **551**, 464–471 (2017).
25. A. C. Komor, Y. B. Kim, M. S. Packer, J. A. Zuris, D. R. Liu, Programmable editing of a target base in genomic DNA without double-stranded DNA cleavage. *Nature* **533**, 420–424 (2016).
26. J. M. Gehrke, O. Cervantes, M. K. Clement, Y. Wu, J. Zeng, D. E. Bauer, L. Pinello, J. K. Joung, An APOBEC3A-Cas9 base editor with minimized bystander and off-target activities. *Nat. Biotechnol.* **36**, 977–982 (2018).
27. A. C. Komor, K. T. Zhao, M. S. Packer, N. M. Gaudelli, A. L. Waterbury, L. W. Koblan, Y. B. Kim, A. H. Badran, D. R. Liu, Improved base excision repair inhibition and bacteriophage Mu Gam protein yields C:G-to-T:A base editors with higher efficiency and product purity. *Sci. Adv.* **3**, eaao4774 (2017).
28. L. L. Lesueur, L. M. Mir, F. M. André, Overcoming the specific toxicity of large plasmids electrotransfer in primary cells in vitro. *Mol. Ther. Nucleic Acids* **5**, e291 (2016).
29. J. N. Søndergaard, K. Geng, C. Sommerauer, I. Atanasoai, X. Yin, C. Kutter, Successful delivery of large-size CRISPR/Cas9 vectors in hard-to-transfect human cells using small plasmids. *Commun. Biol.* **3**, 319 (2020).
30. G. Palermo, Y. Miao, R. C. Walker, M. Jinek, J. A. McCammon, CRISPR-Cas9 conformational activation as elucidated from enhanced molecular simulations. *Proc. Natl. Acad. Sci. U.S.A.* **114**, 7260–7265 (2017).
31. T. Jiang, J. M. Henderson, K. Coote, Y. Cheng, H. C. Valley, X.-O. Zhang, Q. Wang, L. H. Rhym, Y. Cao, G. A. Newby, H. Bihler, M. Mense, Z. Weng, D. G. Anderson, A. P. McCaffrey, D. R. Liu, W. Xue, Chemical modifications of adenine base editor mRNA and guide RNA expand its application scope. *Nat. Commun.* **11**, 1979 (2020).
32. D. Kim, D.-e. Kim, G. Lee, S.-I. Cho, J.-S. Kim, Genome-wide target specificity of CRISPR RNA-guided adenine base editors. *Nat. Biotechnol.* **37**, 430–435 (2019).
33. P. Liang, X. Xie, S. Zhi, H. Sun, X. Zhang, Y. Chen, Y. Chen, Y. Xiong, W. Ma, D. Liu, J. Huang, Z. Songyang, Genome-wide profiling of adenine base editor specificity by EndoV-seq. *Nat. Commun.* **10**, 67 (2019).
34. J. L. Doman, A. Raguram, G. A. Newby, D. R. Liu, Evaluation and minimization of Cas9-independent off-target DNA editing by cytosine base editors. *Nat. Biotechnol.* **38**, 620–628 (2020).
35. Y. K. Jeong, S. Lee, G.-H. Hwang, S.-A. Hong, S. Park, J.-S. Kim, J.-S. Woo, S. Bae, Adenine base editor engineering reduces editing of bystander cytosines. *Nat. Biotechnol.*, (2021).
36. Y. Kim, S.-A. Hong, J. Yu, J. Eom, K. Jang, S. Yoon, D. H. Hong, D. Seo, S.-N. Lee, J.-S. Woo, J. Jeong, S. Bae, D. Choi, Adenine base editing and prime editing of chemically derived hepatic progenitors rescue genetic liver disease. *Cell Stem Cell* , (2021).
37. S. Ling, S. Yang, X. Hu, D. Yin, Y. Dai, X. Qian, D. Wang, X. Pan, J. Hong, X. Sun, H. Yang, S. R. Paludan, Y. Cai, Lentiviral delivery of co-packaged Cas9 mRNA and a Vegfa-targeting guide RNA prevents wet age-related macular degeneration in mice. *Nat. Biomed. Eng.* **5**, 144–156 (2021).
38. Y. Chen, S. Zhi, W. Liu, J. Wen, S. Hu, T. Cao, H. Sun, Y. Li, L. Huang, Y. Liu, P. Liang, J. Huang, Development of highly efficient dual-AAV split adenosine base editor for in vivo gene theraphy. *Small Meth.* **4**, 2000309 (2020).

39. H. Nishimasu, X. Shi, S. Ishiguro, L. Gao, S. Hirano, S. Okazaki, T. Noda, O. O. Abudayyeh, J. S. Gootenberg, H. Mori, S. Oura, B. Holmes, M. Tanaka, M. Seki, H. Hirano, H. Aburatani, R. Ishitani, M. Ikawa, N. Yachie, F. Zhang, O. Nureki, Engineered CRISPR-Cas9 nuclease with expanded targeting space. *Science* **361**, 1259–1262 (2018).
40. Y. K. Jeong, J. Yu, S. Bae, Construction of non-canonical PAM-targeting adenosine base editors by restriction enzyme-free DNA cloning using CRISPR-Cas9. *Sci. Rep.* **9**, 4939 (2019).
41. D. H. Jo, D. W. Song, C. S. Cho, U. G. Kim, K. J. Lee, K. Lee, S. W. Park, D. Kim, J. H. Kim, J.-S. Kim, S. Kim, J. H. Kim, J. M. Lee, CRISPR-Cas9–mediated therapeutic editing of *Rpe65* ameliorates the disease phenotypes in a mouse model of Leber congenital amaurosis. *Sci. Adv.* **5**, eaax1210 (2019).
42. W.-H. Yeh, H. Chiang, H. A. Rees, A. S. B. Edge, D. R. Liu, In vivo base editing of post-mitotic sensory cells. *Nat. Commun.* **9**, 2184 (2018).
43. C.-Q. Song, T. Jiang, M. Richter, L. H. Rhym, L. W. Koblan, M. P. Zafra, E. M. Schatoff, J. L. Doman, Y. Cao, L. E. Dow, L. J. Zhu, D. G. Anderson, D. R. Liu, H. Yin, W. Xue, Adenine base editing in an adult mouse model of tyrosinaemia. *Nat. Biomed. Eng.* **4**, 125–130 (2020).
44. J. M. Levy, W.-H. Yeh, N. Pendse, J. R. Davis, E. Hennessey, R. Butcher, L. W. Koblan, J. Comander, Q. Liu, D. R. Liu, Cytosine and adenine base editing of the brain, liver, retina, heart and skeletal muscle of mice via adeno-associated viruses. *Nat. Biomed. Eng.* **4**, 97–110 (2020).
45. S. Suh, E. H. Choi, H. Leinonen, A. T. Foik, G. A. Newby, W.-H. Yeh, Z. Dong, P. D. Kiser, D. C. Lyon, D. R. Liu, K. Palczewski, Restoration of visual function in adult mice with an inherited retinal disease via adenine base editing. *Nat. Biomed. Eng.* **5**, 169–178 (2020).
46. N. M. Gaudelli, D. K. Lam, H. A. Rees, N. M. Solá-Esteves, L. A. Barrera, D. A. Born, A. Edwards, J. M. Gehrke, S.-J. Lee, A. J. Liquori, R. Murray, M. S. Packer, C. Rinaldi, I. M. Slaymaker, J. Yen, L. E. Young, G. Ciaramella, Directed evolution of adenine base editors with increased activity and therapeutic application. *Nat. Biotechnol.* **38**, 892–900 (2020).
47. S. Kim, T. Koo, H. G. Jee, H. Y. Cho, G. Lee, D. G. Lim, H. S. Shin, J. S. Kim, CRISPR RNAs trigger innate immune responses in human cells. *Genome Res.* **28**, 367–373 (2018).
48. S. W. Park, J. H. Kim, W. J. Park, J. H. Kim, Limbal approach-subretinal injection of viral vectors for gene therapy in mice retinal pigment epithelium. *J. Vis. Exp.* **2015**, e53030 (2015).
49. S. Bae, J. Kweon, H. S. Kim, J.-S. Kim, Microhomology-based choice of Cas9 nuclease target sites. *Nat. Methods* **11**, 705–706 (2014).
50. G.-H. Hwang, J. Park, K. Lim, S. Kim, J. Yu, E. Yu, S.-T. Kim, R. Eils, J.-S. Kim, S. Bae, Web-based design and analysis tools for CRISPR base editing. *BMC Bioinformatics* **19**, 542 (2018).

Acknowledgments

Funding: This work was supported by grants from the National Research Foundation of Korea (NRF) (nos. 2018M3D1A1058826 and 2015M3A7B6027946 to J.H.K.; nos. 2020M3A9I4036074 and 2017R1A6A3A04004741 to D.H.J.; no. 2018R1C1B6004447 to J.-S.W.; and nos. 2021M3A9H3015389, 2020R1A6A1A06046728, and 2020M3A9I4036072 to S.B.), the Technology Innovation Program (no. 20000158) to S.B., and the Korea Research Institute of Bioscience & Biotechnology (KRIBB) Research Initiative Program (KGM5362111) to J.H.K. **Author contributions:** S.B., J.-S.W., and J.H.K. conceived this project; S.-N.L. performed the protein production steps in the human cell system; H.-K.J., Y.K.J., Y.J., and J.Y. performed the experiments and analysis in cells; D.H.J. and C.S.C. performed subretinal injections in mice; H.-K.J., D.H.J., S.-N.L., J.H.K., J.-S.W., and S.B. wrote the manuscript with the approval of all other authors; and J.H.K., J.-S.W., and S.B. supervised the research. **Competing interests:** J.H.K., J.-S.W., and S.B. are filing a patent application based on this work. All other authors declare no competing interests. **Data and materials availability:** All data needed to evaluate the conclusions in the paper are present in the paper and/or the Supplementary Materials.

Submitted 21 December 2020
Accepted 7 July 2021
Published 27 August 2021
10.1126/sciadv.abg2661

Citation: H.-K. Jang, D. H. Jo, S.-N. Lee, C. S. Cho, Y. K. Jeong, Y. Jung, J. Yu, J. H. Kim, J.-S. Woo, S. Bae, High-purity production and precise editing of DNA base editing ribonucleoproteins. *Sci. Adv.* **7**, eabg2661 (2021).